

# Anomalous magnetoresistance in a two-dimensional hole gas

G. M. Gusev, Z. D. Kvon, and V. N. Ovsyuk

*Institute of Semiconductor Physics, Siberian Division, Academy of Sciences of the USSR*

(Submitted 31 October 1984)

*Zh. Eksp. Teor. Fiz.* **88**, 2077–2087 (June 1985)

The anomalous magnetoresistance (AMR) in a two-dimensional hole gas near the (100), (110), and (111) surfaces of silicon is studied. It is shown that the AMR can be described completely if quantum-theoretic corrections to the spin-orbit interaction are included. The energy relaxation time of the two-dimensional holes is found by comparing the experimental and theoretical results. Two mechanisms are responsible for the energy relaxation—elastic electron-electron collisions that conserve the total angular momentum of the system, and inelastic hole-hole collisions with simultaneous scattering by impurities (which change the angular momentum). The investigation of the AMR revealed for the first time a mechanism of spin relaxation in two-dimensional systems. The corresponding relaxation time is calculated for this spin relaxation mechanism in which the spin-orbit interaction in systems without an inversion center lifts the spin degeneracy of the quantum subbands. Information is obtained regarding the energy spectrum of the two-dimensional holes; in particular, the population characteristics of the light-hole subband (which is produced by dimensional quantization) are found for the principal crystallographic surfaces of silicon, and the magnitude of the spin splitting is determined for the first time.

## 1. INTRODUCTION

The discovery of quantum corrections necessitated by localization and interaction effects<sup>1–4</sup> has led to a new area of research in the physics of disordered Fermi systems. In addition to providing a deeper understanding of localization and interaction, the new methods also provide a powerful tool for analyzing electronic processes in these systems. In particular, information about the nature of the interaction and the energy, spin, and intervalley relaxation<sup>5</sup> unobtainable by other means can be gained from studies of the anomalous magnetoresistance (AMR) caused by the dependence of the quantum corrections on the magnetic field.

Two-dimensional electron or hole gases near semiconductor surfaces are of particular interest. This is due in part to the fact that the properties that determine the behavior of the AMR (Fermi energy, impurity density, etc.) can be varied over wide limits, and in part to the detailed information available regarding the energy spectrum, which must be known accurately in order to compare the theoretical and experimental results. Extensive experimental data are available regarding the behavior of the negative AMR in two-dimensional electron gases near silicon surfaces.<sup>6–11</sup> These data confirm virtually all of the theoretical predictions. However, much less work has been done on the AMR in two-dimensional hole gases, although these systems are of interest because the strong spin-orbit interaction alters the quantum corrections.<sup>12–14</sup>

In this paper we report detailed experimental results on the AMR of two-dimensional holes near a silicon surface as a function of the temperature  $T$  and excess surface carrier densities  $n_p$  in a channel for several different surface orientations. We also study how a strong isotropic deformation alters the AMR. Our results support all the basic theoretical predictions for two-dimensional systems with a strong spin-orbit interaction. A comparison of the experimental and

theoretical results yields information on the energy and spin relaxation of the two-dimensional holes, in addition to some new results on the energy spectrum.

## 2. THEORY OF THE AMR IN A TWO-DIMENSIONAL HOLE GAS

### 2.1 Energy spectrum of two-dimensional holes near a silicon surface

One characteristic feature of the energy spectrum of two-dimensional holes in inversion channels in MOS transistors is that dimensional quantization effects remove the degeneracy of the light and heavy hole bands at zero momentum  $k = 0$ . The two-dimensional hole spectrum has been studied both theoretically<sup>15,16</sup> and experimentally (Shubnikov-de Haas oscillations, cyclotron resonance<sup>17–19</sup>). These studies show that the effective mass  $m_p^*$  of the holes is not constant but increases with energy (the spectrum is nonparabolic). The mass  $m_p^*$  also depends on the orientation of the surface at which the two-dimensional holes are generated:  $m_p^*/m_0 = 0.4–0.6$  for the (100) and (111) crystallographic planes, while  $m_p^*/m_0 = 0.3–0.4$  for the (110) surface. The behavior of the Shubnikov-de Haas oscillations also reveals that for  $n_p = 2.5 \cdot 10^{12} \text{ cm}^{-2}$ , the Fermi energy  $E_F$  for holes near the (110) surface crosses the bottom of a second (light-hole) subband which is produced by dimensional quantization of light holes of mass  $0.2m_0$ . No information is available regarding the population of the light-hole subband for the (111) and (100) orientations. We note that in general, the spin degeneracy of the holes should be lifted because of the lack of an inversion center in the potential well near the surface.

### 2.2 Theory of the AMR in a two-dimensional hole gas

Because the spin-orbit interaction is strong in the valence band, we anticipate that the behavior of the AMR in two-dimensional hole gases will be largely determined by the spin relaxation of the holes. Two situations can occur—ei-

TABLE I. Properties of the samples.

| Orientation | $N_A, N_D$<br>$10^{15} \text{ cm}^{-3}$ | Maximum<br>mobility, $\text{cm}^2/\text{V}\cdot\text{s}$<br>(at $T = 4.2 \text{ K}$ ) | Channel<br>length/<br>width<br>ratio | Oxide thick-<br>ness, $\text{\AA}$ | Channel<br>length, $\mu\text{m}$ |
|-------------|---|---|--------------------------------------|------------------------------------|----------------------------------|
| (100)       | 0.2                                     | 1500  | 3                                    | 1500                               | 1200                             |
| (110)       | 0.25                                    | 2500  | 3                                    | 1100                               | 1200                             |
| (111)       | 0.5                                     | 1100  | 3                                    | 1300                               | 1200                             |
| (100)*      | 5                                       | 1500  | 3,6                                  | 1000                               | 1800                             |

\*For inversion channels on 0.5- $\mu\text{m}$ -thick silicon films on sapphire substrates.

ther  $E_F < \Delta$  or  $E_F > \Delta$ , where  $E_F$  is the Fermi energy of the holes and  $\Delta$  is the splitting of the heavy- and light-hole bands. In the first case, spin relaxation proceeds by the D'yakonov-Perel' mechanism,<sup>20</sup> because the spin degeneracy of the fundamental (heavy-hole) subband is lifted; spin-orbit scattering by impurities also plays a role.<sup>3</sup> The AMR experiments in two-dimensional electron gases<sup>6-11</sup> show that spin-orbit scattering by impurities does not occur in the Si-SiO<sub>2</sub> system, so that the latter mechanism may be neglected. The expression for the magnetoconductivity then takes the form

$$\Delta G(H) = -\frac{e^2}{2\pi^2\hbar} \left[ -\frac{3}{2} f(x^*) + \left( \frac{1}{2} + \beta(T) \right) f(x) \right], \quad (1)$$

where

$$x = \frac{4DeH}{\hbar c} \tau_\varphi, \quad x^* = \frac{4DeH}{\hbar c} \tau_\varphi^*,$$

$$(\tau_\varphi^*)^{-1} = \tau_\varphi^{-1} + 1/3 \tau_{so}^{-1}, \quad f(x) = \ln x + \psi(1/2 + 1/x);$$

here  $\psi(x)$  is the logarithmic derivative of the gamma-function,  $D$  is the diffusion coefficient, the factor  $\beta(T)$  reflects the effects of the magnetic field on the scattering by superconducting fluctuations,<sup>21</sup>  $\tau_\varphi$  is the phase relaxation time of the wave function due to inelastic collisions, and  $\tau_{so}$  is the spin relaxation time.

On the other hand, if  $E_F > \Delta$  then the spin relaxation is caused primarily by carrier transitions between the light- and heavy-hole subbands. In this case  $\tau_{so} \sim \tau_p \ll \tau_\varphi$  and the magnetoconductivity is given by

$$\Delta G(H) = -\frac{e^2}{2\pi^2\hbar} \left[ \frac{1}{2} + \beta(T) \right] f(x). \quad (2)$$

We note that (1) and (2) do not contain any terms associated with fluctuation interactions<sup>5</sup> or Zeeman splitting,<sup>22</sup> because these effects were negligible under the experimental conditions.

### 3. EXPERIMENTAL METHOD

We studied the magnetoresistance of  $p$ -channel MIS transistors fabricated by conventional planar technology on (100), (110), and (111) silicon substrates. Table I summarizes the basic properties of the samples.

The measurements were carried out by a null method using a dc current; the field was less than 0.1 V/cm inside the samples, so that carrier heating was negligible. We used potentiometric probes to eliminate any possible contact effects,

even though none was noted for the experimental range of magnetic fields  $H \leq 3 \text{ kG}$ . The measurements were carried out for  $T = 1.6\text{--}4.2 \text{ K}$  and excess hole densities  $n_p = (1\text{--}9) \cdot 10^{12} \text{ cm}^{-2}$  at the surface of the channel. The hole excess was calculated from the formula  $n_p = C(V_g - V_t)/e$ , where  $C$  is the capacitance of the oxide layer,  $V_g$  is the gate voltage, and  $V_t$  is the transistor threshold voltage at  $T = 77.3 \text{ K}$ . The above range of  $n_p$  corresponds to  $k_F l = 10\text{--}15$ , i.e., the basic assumption underlying the theory in Ref. 5 was well satisfied for our samples (here  $k_F$  is the Fermi wave vector and  $l$  is the mean free path). We deduced the hole diffusion coefficient (needed to calculate  $\tau_\varphi$  and  $\tau_{so}$ ) from the measured values of the conductivity  $G$  of the inversion layer together with the Einstein relation

$$G = e^2 N D \quad (3)$$

for a degenerate system (here  $N = m_p^* / \pi \hbar^2$  is the density of states). The values for the effective mass  $m_p^*$  given in Ref. 19 were found by analyzing the cyclotron resonance of the two-dimensional holes; they are the most accurate available and will be used here. Since the hole spectrum in nonparabolic, the state density in this case depends on the energy; we therefore found  $E_F$  by graphically integrating the dependence  $m_p^*(n_p)$  found in Ref. 19.

### 4. EXPERIMENTAL RESULTS

A positive AMR was observed in all the samples, regardless of surface orientation. Figure 1 shows the depen-

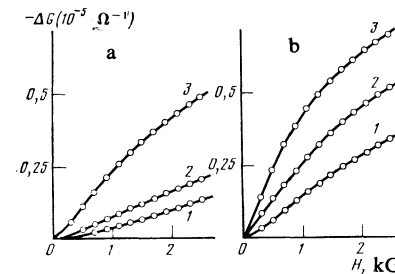


FIG. 1. Field dependence of the magnetoresistance of an inversion channel on a (111) silicon surface. a:  $T = 1.7 \text{ K}$ ,  $n_p = 1.3 \cdot 10^{12} \text{ cm}^{-2}$  (1),  $1.6 \cdot 10^{12} \text{ cm}^{-2}$  (2),  $2.5 \cdot 10^{12} \text{ cm}^{-2}$  (3). The solid curve shows experimental results, the open circles give values found by Eq. (1) for  $\tau_\varphi = 6, 8,$  and  $12 \text{ ps}$  and  $\tau_{so} = 1.6, 1.05, 0.8 \text{ ps}$ , respectively. b:  $n_p = 4.45 \cdot 10^{12} \text{ cm}^{-2}$ ,  $T = 4.2$  (1),  $2.6$  (2),  $1.7 \text{ K}$  (3). The solid curves show experimental results, the open circles give values from Eq. (1) for  $\tau_\varphi = 7, 12,$  and  $21.5 \text{ ps}$ ,  $\tau_{so} = 0.7$ .

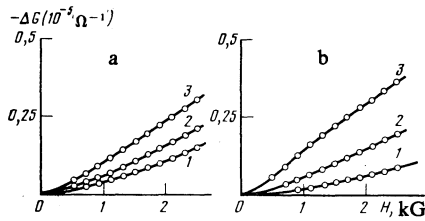


FIG. 2. Field dependence for a (100) silicon surface. a:  $T = 1.7$  K,  $n_p = 1.3 \cdot 10^{12}$   $\text{cm}^{-2}$  (1),  $1.6 \cdot 10^{12}$   $\text{cm}^{-2}$  (2),  $2.5 \cdot 10^{12}$   $\text{cm}^{-2}$  (3). The solid curves give experimental results, the open circles show values calculated from Eq. (2) for  $\tau_\varphi = 3.2, 3.7, 4.9$  ps; b:  $n_p = 4.4 \cdot 10^{12}$   $\text{cm}^{-2}$ ,  $T = 4.2$  (1),  $2.6$  (2),  $1.7$  K (3). The solid curve shows experimental values, the open circles give the values from Eq. (2) for  $\tau_\varphi = 1.7, 3.2,$  and  $6.3$  ps.

dence of the magnetoconductance  $\Delta G(H)$  on the magnetic field at  $T = 1.7$  K for three hole densities (a) and for  $n_p = \text{const}$  as  $T$  decreased (b) for the (111) orientation. We see that  $-\Delta G$  was negative (i.e., the magnetoresistance was positive); the initial quadratic increase of  $\Delta G$  with  $H$  became less rapid for higher  $H$ . The range of fields for which  $\Delta G \sim H^2$  became narrower as  $1/T$  and  $n_p$  increased, and for  $n_p = 2.4 \cdot 10^{12}$   $\text{cm}^{-2}$  and  $T = 1.7$  K no region with  $\Delta G \sim H^2$  is discernible to the scale shown in Fig. 1. For  $H = \text{const}$ , on the other hand,  $|\Delta G|$  increased with  $n_p$  and/or  $1/T$ . According to Fig. 2a, b the dependence  $\Delta G(H)$  for a (100) surface was similar; however,  $|\Delta G|$  was somewhat smaller in this case and the dependence was quadratic for a wider range of  $H$ .

We will show in the next section that for the (111) orientation, only the lowest (heavy-hole) quantum subband is filled even for concentrations as high as  $n_p = 5.5 \cdot 10^{12}$   $\text{cm}^{-2}$ . In this case we can use relation (1) to compare the theory with experiment. The open circles in Fig. 1a, b show  $\Delta G(H)$  calculated from Eq. (1) for the parameter value indicated in the caption. The experimental and calculated results are in complete agreement. For  $H = \text{const}$ ,  $|\Delta G|$  increases with  $n_p$  and  $1/T$  because the characteristic time  $\tau_\varphi$  increases. Figure 3a shows the dependence  $\tau_\varphi(T)$  deduced by comparing the experimental results with Eq. (1); we see that  $\tau_\varphi$  is proportional to  $T^{-p}$ . The mechanism responsible for the phase relaxation of the hole wave function will be discussed below. Because of the appreciable experimental error and the presence of several adjustable parameters in the equations, we cannot conclude that hole scattering by superconducting fluctuations does not contribute to the magnetoresistance,

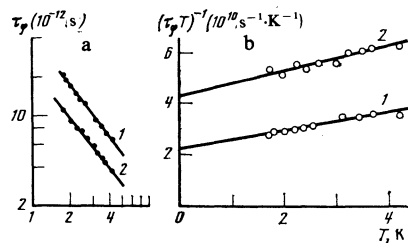


FIG. 3. a: dependence  $\tau_\varphi(T)$  for  $n_p = 4.4 \cdot 10^{12}$   $\text{cm}^{-2}$  (1) and  $1.8 \cdot 10^{12}$   $\text{cm}^{-2}$  (2). b: temperature dependence of  $(\tau_\varphi T)^{-1}$  for  $n_p = 4.4 \cdot 10^{12}$   $\text{cm}^{-2}$  (1) and  $1.8 \cdot 10^{12}$   $\text{cm}^{-2}$  (2).

i.e., that  $\beta(T) = 0$ . However, the agreement between the theoretical and experimental results deteriorates if this contribution is taken to exceed 10% of the total magnetoresistance. It should be noted here that the value of  $\tau_\varphi$  found by comparing theory and experiment will not change by more than 10% if we include the Maki-Thompson corrections.

Analysis of the experimental results for a two-dimensional hole gas on a (100) surface shows that they are accurately described by Eq. (2) with  $\beta \ll 0.1$ , i.e., in this case we have  $\tau_{s0} \sim \tau_\varphi$ , which implies that  $E_F > \Delta$ . Comparison of the theoretical equations (1), (2) with the experimental results (Fig. 2) shows that  $\Delta G(H)$  behaves differently for the (100) and (111) orientations because  $L_\varphi = (D\tau_\varphi)^{1/2}$  was 70% larger for the (111) surface, although the mobility and effective carrier mass were almost identical. This difference in the characteristic lengths  $L_\varphi$  also suggests that the heavy- and the light-hole subbands were both filled in a (100) inversion channel even for  $n_p$  as low as  $\approx 10^{12}$   $\text{cm}^{-2}$  [recall that only the heavy-hole subband was filled for the (111) channel]. Since the density of states is then roughly 50% greater than when only a single subband as filled, the hole diffusion coefficient, the phase relaxation time  $\tau_\varphi$ , and hence also  $L_\varphi$  are several times smaller than for the (111) orientation.

The magnetoresistance and the measured length  $L_\varphi$  for inversion channels on a (110) surface also yield information about the population characteristics of the higher-lying light-hole subband. We will discuss this in the next section.

## 5. ANOMALOUS MAGNETORESISTANCE CAUSED BY OVERLAP OF THE FERMI LEVEL WITH THE LIGHT-HOLE SUBBAND

The case of a (110) silicon surface was discussed in Sec. 2, where we found that the second quantum subband (produced by dimensional quantization of the light holes) begins to fill once  $n_p$  reaches  $2.5 \cdot 10^{12}$   $\text{cm}^{-2}$ . Clearly, this filling should appreciably alter the behavior of the AMR by changing the parameter  $L_\varphi^2 = D\tau_\varphi$ . Figure 4a shows the depen-

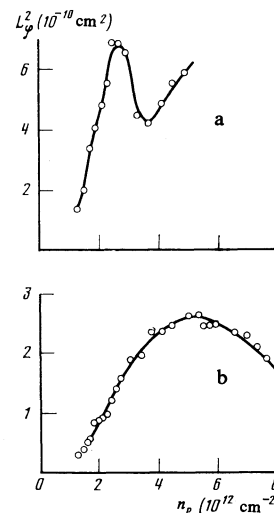


FIG. 4. a: The dependence  $L_\varphi^2(n_p)$  for a (110) silicon surface at  $T = 1.7$  K. b:  $L_\varphi^2(n_p)$  for (111) silicon at  $T = 1.7$  K.

dence  $L_{\varphi}^2(n_p)$  (found by measuring the AMR for two-dimensional holes near a (110) surface. We see that  $L_{\varphi}^2$  increases steadily with  $n_p$  for  $n_p \leq 2 \cdot 10^{12}$ , which is consistent with filling of the fundamental (heavy-hole) subband. However,  $L_{\varphi}^2$  starts to decrease abruptly at  $n_p = 2.5 \cdot 10^{12} \text{ cm}^{-2}$ , passes through a minimum, and then starts to rise again. We can explain this behavior by assuming that the Fermi level rises into the light-hole subband; in this case the density of Fermi-level states should suddenly increase by  $\approx 50\%$  when  $E_F$  crosses the bottom of the second subband, and this will be reflected in a drop in  $\tau_{\varphi}$ ,  $D$ , and  $L_{\varphi}^2$ . We note that  $L_{\varphi}^2(n_p)$  peaks at the value of  $n_p$  at which the Fermi level crosses the bottom of the light-hole subband, as determined from measurements of the conductivity and the Shubnikov–de Haas oscillations. The results are similar for the (111) orientation (Fig. 4b); in this case, however,  $L_{\varphi}^2(n_p)$  peaks at  $n_p = 5.5 \cdot 10^{12} \text{ cm}^{-2}$ , which indicates that the light-hole subband starts to fill only after higher concentrations have been reached.<sup>14</sup> We did not observe any peaks or valleys in  $L_{\varphi}^2(n_p)$  near the (100) surface for  $n_p = (1-9) \cdot 10^{12} \text{ cm}^{-2}$ . This finding again suggests that the subbands for the (100) orientation were filled even for  $n_p \approx 10^{12} \text{ cm}^{-2}$ , as we concluded in the previous section.

## 6. PHASE RELAXATION TIME OF THE WAVE FUNCTION IN A TWO-DIMENSIONAL HOLE GAS

The AMR measurements shown in Fig. 3a reveal that  $\tau_{\varphi}$  increases as  $\sim T^{-p}$  for a (111) surface, where  $p = 1.4$ ; moreover,  $\tau_{\varphi}$  also increases with  $n_p$ . This indicates that hole-hole collisions are primarily responsible for phase relaxation in the two-dimensional hole gas. The value  $p = 1.4$  demonstrates that there are two ‘‘Landau’’ and ‘‘impurity’’ relaxation channels, which involve large and small momentum transfers, respectively. We can then write

$$\tau_{\varphi}^{-1} = AT + BT^2. \quad (4)$$

Expression (4) shows that the exponent  $p$  in  $\tau_{\varphi} \propto T^{-p}$  should be determined by two independent energy relaxation mechanisms with different temperature dependences. This can be verified by extrapolating the experimental dependence

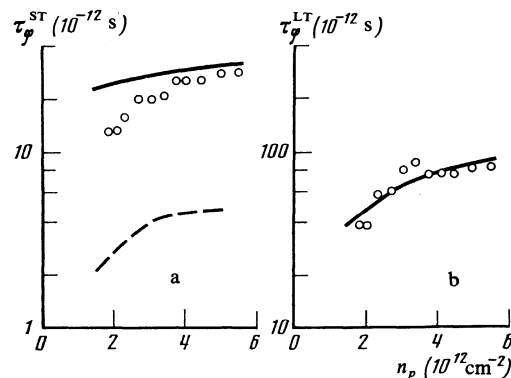


FIG. 5. a: The dependence  $\tau_{\varphi}^{\text{ST}}(n_p)$ . The circles show experimental results, the solid and dashed curves were calculated from Eqs. (5) and (6), respectively. b:  $\tau_{\varphi}^{\text{LT}}(n_p)$ ; the solid curve was calculated from Eq. (7) with  $C = 1.4$ , the open circles show experimental values.

( $\tau_{\varphi} T$ )<sup>-1</sup> to  $T = 0$ ; A should then be equal to ( $\tau_{\varphi} T$ )<sup>-1</sup> (0). Figure 3b shows that the experimental ( $\tau_{\varphi} T$ )<sup>-1</sup> dependence is in fact linear. A similar extrapolation procedure can be used to find the magnitude of each contribution to  $\tau_{\varphi}$ . Figure 5a shows how the relaxation time  $\tau_{\varphi}^{\text{ST}} = (AT)^{-1}$  at  $T = 1.7 \text{ K}$  depends on the surface excess hole concentration;  $\tau_{\varphi}^{\text{ST}}$  represents the contribution to  $\tau_{\varphi}$  from the impurity mechanism (i.e., associated with scattering by static defects such as impurities or rough spots, which promote hole collisions with a small momentum transfer). Two different theoretical expressions have been derived for  $\tau_{\varphi}^{\text{ST}}$ ; according to Ref. 23,

$$(\tau_{\varphi}^{\text{ST}})^{-1} = \frac{e^2 kT}{2\pi \hbar^2 G} \ln \frac{\pi \hbar G}{e^2}; \quad (5)$$

while Refs. 24 and 25 give

$$(\tau_{\varphi}^{\text{ST}})^{-1} = \frac{e^2 kT}{2\pi \hbar^2 G} \ln \frac{T_1}{T}, \quad (6)$$

$$T_1 = 4\hbar (E_F \tau_p / \hbar)^2 D \kappa^2, \quad \kappa = 2\pi N e^2 / \epsilon^*,$$

$$\epsilon^* = (\epsilon_{\text{S1}} + \epsilon_{\text{S1}\alpha}) / 2 = 7.6.$$

These expressions are clearly fundamentally different, since one predicts that  $\tau_{\varphi}^{\text{ST}} \propto T^{-1}$  while the other gives  $\tau_{\varphi}^{\text{ST}} \propto T^{-1} \ln T$ . Figure 5a plots the dependences  $\tau_{\varphi}^{\text{ST}}(n_p)$  given by (5) and (6); clearly, Eq. (5) describes the experimentally measured time  $\tau_{\varphi}^{\text{ST}}$  more accurately than Eq. (6), which gives values nearly an order of magnitude too low. The error in determining the ‘‘effective mass of the density of states’’ is probably responsible for the discrepancy observed for  $n_p \leq 3 \cdot 10^{12} \text{ cm}^{-2}$ . We note that Eq. (5) also correctly describes the time  $\tau_{\varphi}^{\text{ST}}$  measured in two-dimensional electron gases.<sup>26,27</sup>

Figure 5b presents some experimental results for  $\tau_{\varphi}^{\text{LT}} = (BT^2)^{-1}$ , which represents the contribution to  $\tau_{\varphi}$  from the Landau mechanism, i.e., from collisions with large momentum transfers  $\sim k_F$ . The theory in Refs. 28 and 29 gives the expression

$$(\tau_{\varphi}^{\text{LT}})^{-1} = C \frac{(kT)^2}{E_F \hbar} \ln \frac{E_F}{kT} \quad (7)$$

for the two-dimensional case; here the coefficient  $C$  is insensitive to  $E_F$ . Since  $\tau_{\varphi}^{\text{LT}}$  cannot be measured accurately enough to pick up the weak logarithmic dependence on  $T$ , we have retained only the linear and quadratic terms in  $T$  in Eq. (4). Figure 5b shows how the calculated and experimental values of  $\tau_{\varphi}^{\text{LT}}$  depend on  $n_p$ ; Eq. (7) with  $C = 1.4$  is seen to describe the experimental results satisfactorily. The same value  $C = 1.4$  is also found from energy relaxation studies for two-dimensional electron gases.<sup>26,27</sup>

## 7. ANOMALOUS MAGNETORESISTANCE AND SPIN RELAXATION IN A TWO-DIMENSIONAL HOLE GAS

Carrier transitions from the heavy to the light hole bands and/or the D’yakonov-Perel’ mechanism may be responsible for spin relaxation in a two-dimensional hole gas (see Sec. 2 above). Our analysis of the experimental results (Secs. 4, 5) showed that the light-hole subband starts to fill up at  $n_p = 2.5 \cdot 10^{12} \text{ cm}^{-2}$  and  $n_p = 5.5 \cdot 10^{12} \text{ cm}^{-2}$  for the (110)

and (111) orientations, respectively, whereas both subbands are filled for a (100) surface even for  $n_p = 1 \cdot 10^{12} \text{ cm}^{-2}$ , the lowest concentration in the experiment. In this case, scattering of holes from one subband to the other results in rapid relaxation of the hole spins during times  $\tau_{s0} \sim \tau_p$ . Thus if  $E_F < \Delta$ , the D'yakonov-Perel' mechanism<sup>20</sup> is solely responsible for the spin relaxation, i.e., the relaxation is due to splitting of the subbands by the spin-orbit interaction in the MIS inversion channel, which lacks an inversion center. Some consequences of this splitting were recently investigated in Refs. 30–32 for GaAs-AlGaAs heterostructures.

In general it is difficult to distinguish these two spin relaxation mechanisms, because  $E_F$  lies a distance  $\ll \hbar/\tau_p$  from the bottom of the light-hole subband before the latter starts to fill, and this situation is almost impossible to analyze theoretically. In addition, the experimentally measured time  $\tau_{s0}$  was just 3–4 times greater than the momentum relaxation time and therefore could not be measured accurately. The energy distance between the subbands must be increased if the spin relaxation processes are to be examined in detail. The increased spacing will then eliminate the interband scattering processes, and the spin will relax more slowly so that  $\tau_{s0}$  can be measured. This situation occurs in inversion channels in silicon-on-sapphire MIS transistors, where the compressive strain in the silicon films increases the energy gap between the subbands severalfold. Figure 6a shows how the magnetoresistance (MR) of an inversion channel in silicon-on-sapphire depends on  $H$  for three excess concentrations  $n_p$  at the surface. For small  $n_p$ , we see that  $-\Delta G$  is positive for all  $H$  (i.e., the MR is negative). As  $n_p$  increases,  $-\Delta G$  increases for small  $H$  but then passes through a maximum and becomes negative ( $n_p = 1.6 \cdot 10^{12} \text{ cm}^{-2}$ ). Finally, for  $n_p = 2 \cdot 10^{12} \text{ cm}^{-2}$   $-\Delta G$  is negative for all  $H$ . Similar behavior is found for  $n_p = \text{const}$  when  $T$  varies; Fig. 6b shows  $\Delta G(H)$  for  $T = 3.4, 2.05,$  and  $1.6 \text{ K}$ . We see that  $-\Delta G$  remains positive longer as  $T$  drops, i.e., the field  $H_0$  at which

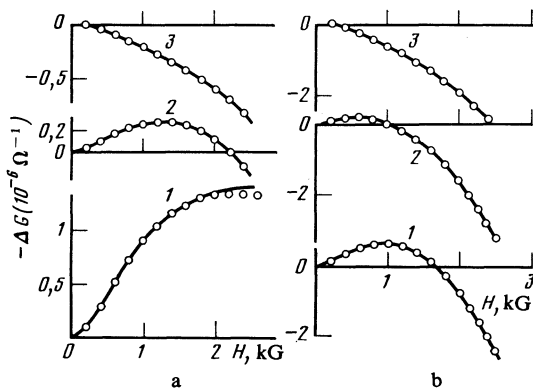


FIG. 6. Field dependence of the magnetoresistance of an inversion channel on a (100) silicon-on-sapphire surface. a:  $T = 1.7 \text{ K}$ ,  $n_p = 2.3 \cdot 10^{12} \text{ cm}^{-2}$  (1),  $1.6 \cdot 10^{12} \text{ cm}^{-2}$  (2),  $1.3 \cdot 10^{12} \text{ cm}^{-2}$  (3). The solid curves plot the experimental results, the circles give values from Eq. (1) for  $\tau_\varphi = 7.7, 5.4,$  and  $4.2 \text{ ps}$ ,  $\tau_{s0} = 2.3, 4.1, 5.4 \text{ ps}$ , respectively. b:  $n_p = 1.4 \cdot 10^{12} \text{ cm}^{-2}$ ,  $T = 1.6$  (1),  $2.05$  (2),  $3.4 \text{ K}$  (3). The solid curves give experimental values; the circles show values calculated from Eq. (1) for  $\tau_\varphi = 4.1, 3.4, 1.2 \text{ ps}$  and  $\tau_{s0} = 5.2, 5.1, 5.4 \text{ ps}$ , respectively.

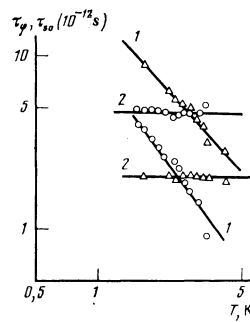


FIG. 7.  $\tau_\varphi$  (1) and  $\tau_{s0}$  (2) as functions of temperature. The symbols  $\circ$  and  $\triangle$  show values for  $n_p = 1.4 \cdot 10^{12} \text{ cm}^{-2}$  and  $n_p = 2.55 \cdot 10^{12} \text{ cm}^{-2}$ , respectively.

$\Delta G$  vanishes increases with  $1/T$ . We can describe this theoretically by assuming that the magnetic field suppresses the contribution to the conductivity from the Anderson localization that accompanies the relaxation of the hole spins. In this case, (1) implies that  $\tau_{s0} > \tau_\varphi$  for small  $n_p$ , and the MR is negative. The spin relaxation rate and the time  $\tau_\varphi$  increase with  $n_p$  (Ref. 12), so that  $\tau_{s0} < \tau_\varphi$  for larger  $n_p$  and the magnetoresistance becomes positive. For  $n_p = \text{const}$ ,  $\tau_\varphi$  increases appreciably with  $1/T$  whereas  $\tau_{s0}$  remains unchanged. Thus, although  $\tau_{s0} > \tau_\varphi$  at  $T = 4.2 \text{ K}$ , the inequality is reversed at lower  $T$  and the MR becomes positive. This situation can be altered as follows: we can keep  $T$  constant, change the gate voltage so as to decrease  $\tau_{s0}$ , and increase  $n_p$ ; or we can keep  $n_p$  constant in the channel, and increase  $\tau_\varphi$  by cooling the sample. In either case, the MR will change sign from negative to positive. The open circles in Fig. 6a, b show the theoretical values of  $\Delta G(H)$  calculated from (1) for the values of  $\tau_\varphi$  and  $\tau_{s0}$  indicated in the caption; the theoretical and experimental values are seen to agree closely. Figure 7 plots  $\tau_\varphi$  and  $\tau_{s0}$ , found by comparing the experimental and theoretical results, as a function of  $T$  for two cases: 1)  $n_p = 1.4 \cdot 10^{12} \text{ cm}^{-2}$  (in this case  $\tau_{s0} > \tau_\varphi$  for all  $T$  in the experimental range); 2)  $n_p = 2.55 \cdot 10^{12} \text{ cm}^{-2}$  (in this case,  $\tau_{s0} < \tau_\varphi$  for all  $T$ ). Once again, we see that  $\tau_\varphi \propto T^{-p}$ , just as for the unstrained samples. The values  $\tau_\varphi, L_\varphi$  for a (100) silicon-on-sapphire surface were somewhat higher than for unstrained (100) surfaces, even though the mobilities were almost identical in both cases. This again confirms

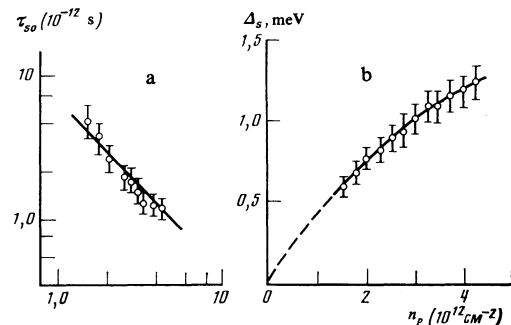


FIG. 8. a:  $\tau_{s0}(n_p)$ ; b:  $\Delta_s(n_p)$ .

that the heavy- and light-hole subbands were both filled in the unstrained (100) samples.

Figure 7 shows that the spin relaxation time is independent of temperature (as expected for a degenerate gas). We measured  $\tau_{s0}$  as a function of  $n_p$  in order to examine the spin relaxation mechanism in more detail. The results (Fig. 8a) show that  $\tau_{s0}$  dropped abruptly as  $n_p$  increased. If  $(\Delta_s \tau_p)/\hbar \ll 1$ , the theory gives the expression

$$\tau_{s0}^{-1} = a (\Delta_s / \hbar)^2 \tau_p \quad (8)$$

for spin relaxation by the D'yakonov-Perel' mechanism<sup>20</sup>; here  $\Delta_s$  is the magnitude of the spin splitting,  $\tau_p$  is the momentum scattering time, and the coefficient  $a$  depends on the scattering mechanism ( $a = 1$  for a short-range potential). Figure 8b shows the dependence  $\Delta_s(n_p)$  calculated from Eq. (8), with  $\tau_{s0}(n_p)$  and  $\tau_p$  deduced from the AMR and conductance measurements, respectively. Clearly,  $\Delta_s$  increases with  $n_p$ . Although this agrees with the calculated results in Ref. 15, the magnitude of  $\Delta_s$  deduced from the measurements is just one-third of the calculated splitting. Because no method is presently available for accurately calculating the energy spectrum of the two-dimensional holes, there is little to be gained by pursuing this discrepancy further. A more detailed analysis will require further theoretical and experimental work for systems which possess a spin-orbit interaction but no inversion center.

## 8. CONCLUSIONS

The anomalous magnetoresistance observed in two-dimensional hole gases on silicon surfaces is accurately described by a theory that allows for dimensional quantization (localization) effects in systems with a strong spin-orbit interaction. The energy relaxation time of the two-dimensional holes can be found as a function of temperature and excess hole concentration by comparing the experimental and theoretical results. Analysis of these dependences shows that the energy relaxation is due to inelastic hole-hole collisions (plus elastic scattering by static defects). Our study of the spin relaxation time  $\tau_{s0}$  has revealed a novel mechanism in which the spin-orbit interaction lifts the spin degeneracy in systems without an inversion center. Analysis of the anomalous magnetoresistance also provides information on the energy spectrum of two-dimensional holes that cannot be obtained by other means. In particular, we have obtained new information about how the higher (light-hole) subband is filled for the principal (100), (110), and (111) silicon faces.

In conclusion, we thank B. L. Al'tshuler, A. G. Aronov, and D. E. Khmel'nitskiĭ for numerous helpful discussions,

M. V. Éntin and A. M. Palkin for helpful remarks, and I. G. Neizvestnyi for his interest and encouragement.

- <sup>1</sup>E. Abrahams, P. W. Anderson, D. C. Liccardello, and T. V. Ramakrishnan, *Phys. Rev. Lett.* **42**, 673 (1979).
- <sup>2</sup>L. P. Gor'kov, A. I. Larkin, and D. E. Khmel'nitskiĭ, *Pis'ma Zh. Eksp. Teor. Fiz.* **30**, 248 (1979) [*JETP Lett.* **30**, 228 (1979)].
- <sup>3</sup>S. Hikami, A. I. Larkin, and Y. Nagaoka, *Prog. Theor. Phys.* **63**, 707 (1980).
- <sup>4</sup>B. L. Altshuler, A. G. Aronov, and P. A. Lee, *Phys. Rev. Lett.* **44**, 1278 (1980).
- <sup>5</sup>B. L. Al'tshuler, A. G. Aronov, A. I. Larkin, and D. E. Khmel'nitskiĭ, *Zh. Eksp. Teor. Fiz.* **81**, 768 (1981) [*Sov. Phys. JETP* **54**, 411 (1981)].
- <sup>6</sup>Y. Kawaguchi and S. Kawaji, *Surf. Sci.* **113**, 505 (1982).
- <sup>7</sup>Yu. S. Zinchik, S. V. Kozyrev, and T. A. Polyanskaya, *Pis'ma Zh. Eksp. Teor. Fiz.* **33**, 278 (1981) [*JETP Lett.* **33**, 262 (1981)].
- <sup>8</sup>R. G. Wheeler, *Phys. Rev. B* **24**, 4645 (1982).
- <sup>9</sup>D. J. Bishop, R. C. Dynes, and D. S. Tsui, *Phys. Rev. B* **26**, 773 (1982).
- <sup>10</sup>M. J. Uren, R. A. Davies, M. Kaveh, and M. Pepper, *J. Phys. C: Sol. St. Phys.* **14**, 5737 (1981).
- <sup>11</sup>G. M. Gusev, Z. D. Kvon, and V. N. Ovsyuk, *Fiz. Tverd. Tela (Leningrad)* **25**, 2776 (1983) [*Sov. Phys. Solid State* **25**, 1599 (1983)].
- <sup>12</sup>G. M. Gusev, Z. D. Kvon, I. G. Neizvestnyi, V. N. Ovsyuk, and A. M. Palkin, *Pis'ma Zh. Eksp. Teor. Fiz.* **35**, 206 (1982) [*JETP Lett.* **35**, 256 (1982)].
- <sup>13</sup>G. M. Gusev, Z. F. Kvon, I. G. Neizvestnyi, and V. N. Ovsyuk, *Surf. Sci.* **142**, 73 (1984).
- <sup>14</sup>G. M. Gusev, Z. D. Kvon, I. G. Neizvestnyi, and V. N. Ovsyuk, *Sol. St. Comm.* **46**, 169 (1983).
- <sup>15</sup>F. J. Ohkawa and H. Uemura, *Prog. Theor. Phys. Suppl.* **57**, 164 (1974).
- <sup>16</sup>E. Bangert, K. von Klitzing, and G. Landwehr, in: *Proc. Twelfth Int. Conf. Phys. Semicond.* (M. H. Pilkuhn, ed.), Teubner, Stuttgart (1974), p. 714.
- <sup>17</sup>K. von Klitzing, G. Landwehr, and G. Dorda, *Sol. St. Comm.* **14**, 387 (1974).
- <sup>18</sup>K. von Klitzing, G. Landwehr, and G. Dorda, *Sol. St. Comm.* **15**, 489 (1974).
- <sup>19</sup>J. P. Kotthaus and R. Ranvaud, *Phys. Rev. B* **15**, 5758 (1977).
- <sup>20</sup>M. I. D'yakonov and V. I. Perel', *Zh. Eksp. Teor. Fiz.* **60**, 1954 (1971) [*Sov. Phys. JETP* **33**, 1053 (1971)].
- <sup>21</sup>A. I. Larkin, *Pis'ma Zh. Eksp. Teor. Fiz.* **31**, 239 (1980) [*JETP Lett.* **31**, 219 (1980)].
- <sup>22</sup>P. A. Lee and T. V. Ramakrishnan, *Phys. Rev. B* **26**, 4009 (1982).
- <sup>23</sup>B. L. Altshuler, A. G. Aronov, and D. E. Khmel'nitskiĭ, *J. Phys. C: Sol. St. Phys.* **16**, 7367 (1982).
- <sup>24</sup>E. Abrahams, P. V. Anderson, P. A. Lee, and T. V. Ramakrishnan, *Phys. Rev. B* **24**, 6783 (1981).
- <sup>25</sup>H. Fukuyama and E. Abrahams, *Phys. Rev. B* **27**, 5976 (1983).
- <sup>26</sup>R. A. Davies and M. Pepper, *J. Phys. C: Sol. St. Phys.* **16**, L353 (1983).
- <sup>27</sup>K. K. Choi, *Phys. Rev. B* **28**, 5774 (1983).
- <sup>28</sup>G. F. Giuliani and J. J. Quinn, *Phys. Rev. B* **26**, 4421 (1982).
- <sup>29</sup>A. V. Chaplik, *Zh. Eksp. Teor. Fiz.* **60**, 1845 (1971) [*Sov. Phys. JETP* **33**, 997 (1971)].
- <sup>30</sup>H. L. Stormer, Z. Schlesinger, A. Chang, *et al.*, *Phys. Rev. Lett.* **51**, 126 (1983).
- <sup>31</sup>D. Stein, K. von Klitzing, and G. Wiegmann, *Phys. Rev. Lett.* **51**, 130 (1983).
- <sup>32</sup>Yu. A. Bychkov and É. I. Rashba, *Pis'ma Zh. Eksp. Teor. Fiz.* **39**, 66 (1984) [*JETP Lett.* **39**, 78 (1984)].

Translated by A. Mason